Serological Analysis Identifies Consequential B Cell Epitopes on the Flexible Linker and C-Terminus of Decorin Binding Protein A (DbpA) from *Borrelia burgdorferi*

Elaheh Movahed,[a] David J. Vance,[a] Dylan Ehrbar,[a] Greta Van Slyke,[a] Jennifer Yates,[a] Karen Kullas,[a] Michael Rudolph,[b] Nicholas J. Mantis[a]

aDivision of Infectious Disease, Wadsworth Center, New York State Department of Health, Albany, New York, USA
bNew York Structural Biology Center, New York, New York, USA

Elaheh Movahed and David J Vance contributed equally to this study. Author order was based on alphabetical order of last name.

ABSTRACT Decorin binding protein A (DbpA) is a surface adhesin of *Borrelia burgdorferi*, the causative agent of Lyme disease. While DbpA is one of the most immunogenic of *B. burgdorferi*'s nearly 100 lipoproteins, the B cell epitopes on DbpA recognized by humans following *B. burgdorferi* infection have not been fully elucidated. In this report we profiled ~270 *B. burgdorferi*-seropositive human serum samples for IgM and IgG reactivity with a tiled DbpA 18-mer peptide array derived from *B. burgdorferi sensu stricto* strains B31 and 297. Using enzyme-linked immunosorbent assays (ELISA) and multiplex immunoassays (MIA), we identified 12 DbpA-derived peptides whose antibody reactivities were significantly elevated (generally <10-fold) in *B. burgdorferi*-seropositive sera, compared to those measured in a healthy cohort. The most reactive peptide (>80-fold IgG, 10-fold IgM) corresponded to residues 64 to 81, which map to an exposed flexible loop between DbpA's α-helix 1 and α-helix 2. This loop, whose sequence is identical between strains B31 and 297, overhangs DbpA's substrate binding pocket. A second strongly reactive antibody target (>80-fold IgG, 3 to 5-fold IgM) mapped to DbpA's C-terminus, a lysine rich tail implicated in attachment to glycosaminoglycans. We postulate that antibody responses against these two targets on DbpA could limit *B.burgdorferi*'s ability to attach to and colonize distal tissues during the early stages of infection.

IMPORTANCE The bacterium, *Borrelia burgdorferi*, is the causative agent of Lyme disease, the most reported tick-borne illness in the United States. In humans, clinical manifestations of Lyme disease are complex and can persist for months, even in the face of a robust antibody response directed against numerous *B. burgdorferi* surface proteins, including decorin binding protein A (DbpA), which is involved in the early stages of infection. In this study we employed ~270 serum samples from *B. burgdorferi*-seropositive individuals to better understand human antibody reactivity to specific regions (called epitopes) of DbpA and how such antibodies may function in limiting *B. burgdorferi* dissemination and tissue colonization.

KEYWORDS Lyme disease, antibody, epitope, vaccine, *Borrelia burgdorferi*, antibody function

The bacterium *Borrelia burgdorferi sensu lato* (*B. burgdorferi* s.l.) is the causative agent of Lyme disease (LD) in the Northern Hemisphere, with *Borrelia burgdorferi sensu stricto* (*B. burgdorferi* s.s.) being the most reported tick-borne illness in the United States. In the absence of antibiotic intervention, LD can progress from a localized infection in the first days and weeks following a tick bite to disseminated manifestations (e.g., neuroborreliosis, carditis) and/or Lyme arthritis months or even years later (1).

B. burgdorferi infection is accompanied by a robust, antigen-specific serum IgM and IgG response that arises within days. In fact, LD diagnostics involve tiered IgM and IgG serologic assays to measure reactivity against a combination of *B. burgdorferi* sonicate, *B. burgdorferi* proteins, and/or peptides (2–4). From the standpoint of immunity, *B. burgdorferi*-specific serum antibodies are critical both in clearing *B. burgdorferi* through complement-dependent and complement-independent borreliacidal activities (5–7) and in Fc-mediated opsonophagocytosis (8, 9). However, the specific antibody subsets that contribute to bacterial clearance and the resolution of LD remain unknown (6).

Decorin binding protein A (DbpA; BBA24) is a highly immunoreactive *B. burgdorferi* protein, as evidenced by the appearance of high titer anti-DbpA serum IgG antibodies in the early stages of experimentally infected mice (10, 11), nonhuman primates (12), and human Lyme disease patients (13). Indeed, anti-DbpA IgM and IgG responses have diagnostic value in LD (14). DbpA is a helical, surface-displayed lipoprotein of ~19 kDa that promotes *B. burgdorferi* attachment to connective tissues and components of the extracellular matrix (ECM), including glycosaminoglycans (GAGs), such as decorin, dermatan sulfate, and heparin (15–24). By virtue of its ability to adhere to GAGs, DbpA influences *B. burgdorferi* tropism for specific tissues and cell types (22, 25). DbpA is expressed early during infection and stimulates the onset of antibodies in the absence of CD4 T cell help (26). In a mouse model, anti-DbpA antibodies confer protection against a *B. burgdorferi* challenge by needle injection, although there is some debate as to whether the same holds true in a natural (tick) route of infection (10, 11, 18, 27). Thus, the role of anti-DbpA antibodies in limiting *B. burgdorferi* dissemination and colonization remains unresolved.

Despite DbpA being a primary target of the humoral immune response following *B. burgdorferi*, little is known about the specific epitopes on DbpA recognized by human patients. Arnaboldi and colleagues identified a 15-mer peptide corresponding to N-terminal residues (~6 to 30) of DbpA that was reactive with serum IgM (but not IgG) from early LD patients (28). It should be underscored that those antibody profiles were derived from individuals who had been clinically diagnosed as having erythema migrans (EM), a hallmark of early-stage Lyme disease. Another study identified a DbpA-derived peptide (residues 57–71) reactive with serum IgG antibodies from Lyme neuroborreliosis patients, although the sample size in that study was rather limited (29). Considering DbpA's overall immunogenicity in humans and the fact that B cell epitope prediction tools, such as Bepipred, identify several DbpA peptides with a high propensity to be antibody targets (30, 31), we sought to revisit the question of linear B cell epitopes on DbpA. Addressing this question was possible because we had access to a large collection of de-identified serum samples that had been designated seropositive for *B. burgdorferi* antigens via approved diagnostic tests. While the diagnostic tests are not necessarily indicative of Lyme disease, they do afford a high degree of confidence that an individual had experienced a *B. burgdorferi* infection.

Here, we report the screening of ~270 *B. burgdorferi*-seropositive serum samples against a tiled DbpA 18-mer peptide array derived from *B. burgdorferi* strains B31 and 297. One of the most reactive peptides in our collection (A7) corresponds to the conserved flexible linker that overhangs DbpA's lysine-rich ligand binding pocket. Equally reactive were peptides corresponding to the C-terminal tails of DbpA from B31 and 297, which have also been implicated in substrate recognition. The presence of antibodies targeting these regions of DbpA would be expected to block DbpA-mediated substrate recognition and limit *B. burgdorferi* colonization of distal tissues.

RESULTS

IgM and IgG reactivity with DbpA in *B. burgdorferi*-seropositive serum samples. DbpA is one of the most immunogenic *B. burgdorferi* proteins in humans and nonhuman primates (12, 13, 32–34). To assess the relative reactivity of DbpA in our collection of ~270 clinical samples, serum samples classified as IgM$^+$/IgG$^-$, IgM$^+$/IgG$^+$, and IgM$^-$/IgG$^+$ reactive were subjected to a Luminex analysis with DbpA conjugated microspheres
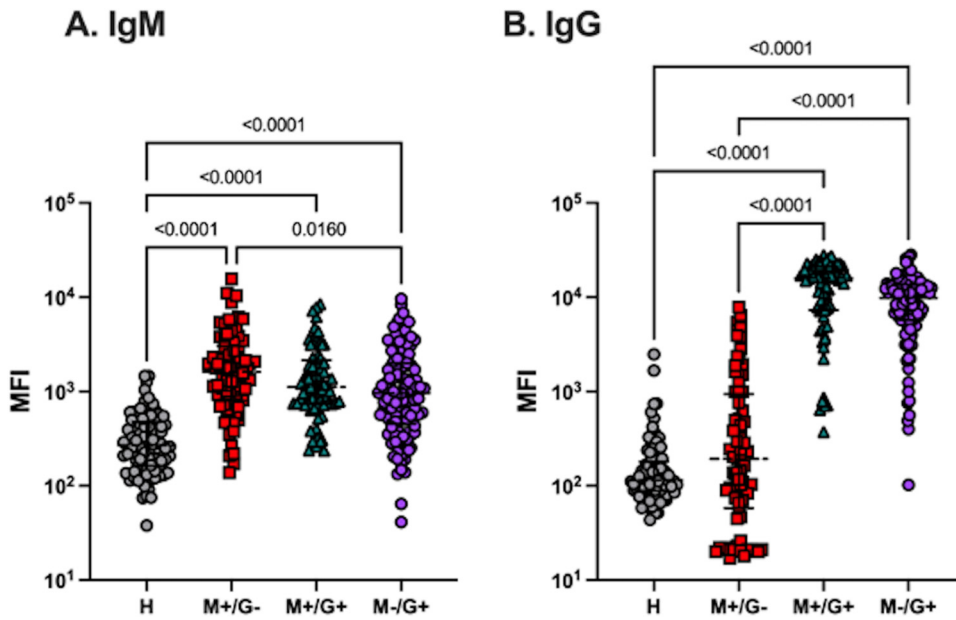
FIG 1 Serum IgM and IgG reactivity with DbpA. Anti-DbpA (A) IgM and (B) IgG reactivity (MFI) in healthy (n = 86) or *B. burgdorferi*-seropositive serum samples, as defined as IgM$^+$/IgG$^-$ (n = 78), IgM$^+$/IgG$^+$ (n = 71), or IgM$^-$/IgG$^+$ (n = 114). Significance was determined by Kruskal-Wallis test with Dunn's post hoc test.

(Fig. 1). Reactivity was compared to a commercial panel of 87 serum samples obtained from healthy individuals.

Within our panel of *B. burgdorferi*-seropositive serum samples, anti-DbpA IgM levels (MFI) in all three clinical cohorts (IgM$^+$/IgG$^-$, IgM$^+$/IgG$^+$, and IgM$^-$/IgG$^+$) were significantly elevated (4 to 7-fold) over those of the healthy controls, with the highest MFIs found in the IgM$^+$/IgG$^-$ group (Fig. 1; Table S1). In the case of IgG, anti-DbpA levels (MFI) were not significantly above those of healthy controls in the IgM$^+$/IgG$^-$ cohort, but they were markedly elevated in the IgM$^+$/IgG$^+$ ($\sim$70-fold) and IgM$^-$/IgG$^+$ ($\sim$50-fold) cohorts (Table 1; Fig. 1). This profile is consistent with the development of DbpA IgM and IgG antibodies that begins in the early stages of *B. burgdorferi* infection. Moreover, on an individual sample basis, anti-DbpA IgG levels were greater than IgM levels in the

TABLE 1 DbpA peptide reactivity with IgG from Lyme disease patient serum samples

		Healthy	IgM+/IgG$^-$			IgM+/IgG+			IgM$^-$/IgG+		
AA^a	#^{b}	MFI (SD)	Index (SD)	MFI (SD)	P value	Index (SD)	MFI (SD)	P value	Index (SD)	MFI (SD)	P value
26-188		205.3 (324.9)	4.2 (7.7)	871.5 (1575)	0.85	68.8 (37.7)^c	14128 (7750)	**<0.0001**	48.2 (28.94)^c	9887 (5940)	**<0.0001**
28-45	B10	94.88 (85.49)	1.6 (3.1)	159.1 (297.2)	>0.99	4.8 (6.8)	452.5 (650.4)	**<0.0001**	3.4 (5.9)	323.5 (563.5)	**<0.0001**
37-54	B11	74.50 (59.93)	4.6 (6.4)	347.0 (481.4)	**<0.0001**	9.1 (12.5)	677.9 (934.0)	**<0.0001**	9.4 (10.86)	704.1 (809.1)	**<0.0001**
46-63	A5	216.0 (467.9)	3.1 (3.8)	686.7 (811.7)	**<0.0001**	8.3 (7.9)	1797 (1717)	**<0.0001**	7.7 (10.34)	1659 (2234)	**<0.0001**
55-72	A6	128.8 (61.46)	0.4 (0.6)	55.36 (79.79)	**<0.0001**	3.4 (7.0)	441.6 (902.5)	0.1801	2.4 (5.3)	304.8 (693.8)	0.2298
	C1	168.9 (115.8)	5.6 (15.8)	944.3 (2675)	**<0.0001**	6.9 (8.5)	1176 (1443)	**<0.0001**	5.7 (8.3)	967.8 (1414)	**<0.0001**
64-81	A7	33.72 (15.07)	2.5 (4.1)	85.67 (137.1)	0.47	84.6 (126.1)^c	2853 (4251)	**<0.0001**	59.7 (86.22)^c	2013 (2907)	**<0.0001**
118-135	B1	174.8 (111.6)	3.7 (4.4)	655.2 (775.8)	**<0.0001**	10.0 (6.5)	1754 (1143)	**<0.0001**	9.5 (8.8)	1658 (1543)	**<0.0001**
136-153	B3	164.6 (352.5)	3.9 (5.9)	644.5 (987.0)	**<0.0001**	7.4 (5.1)	1225 (842.5)	**<0.0001**	7.3 (7.7)	1201 (1276)	**<0.0001**
	C4	71.44 (138.9)	7.2 (9.7)	514.4 (697.1)	**<0.0001**	12.9 (9.4)	924.3 (678.4)	**<0.0001**	15.7 (16.81)	1120 (1201)	**<0.0001**
163-180	C6	29.44 (13.68)	1.3 (2.9)	37.65 (87.01)	0.0098	4.3 (11.8)	127.3 (347.0)	**<0.0001**	3.7 (8.7)	109.8 (257.8)	0.1739
172-189	B7	408.5 (187.7)	0.4 (1.3)	198.3 (551.8)	**<0.0001**	2.9 (5.7)	1213 (2348)	>0.9999	2.9 (5.6)	1194 (2314)	0.0317
	C7	44.28 (30.71)	2.5 (4.2)	108.7 (187.5)	0.79	83.5 (122.1)^c	3698 (5407)	**<0.0001**	58.3 (86.03)^c	2583 (3810)	**<0.0001**

^{a}Amino acid residues. Residues 26-188 (top row) refers to full length recombinant DbpA used in this study that lacks the first 25 residues.
^{b}Peptide names, as noted in Fig. 2. Underlines indicate 297-specific peptides. P values were derived from Dunn's multiple comparison tests following Kruskal-Wallis tests.
^{c}Peptides with index values >20.

A.

B. B31 [2LQU]

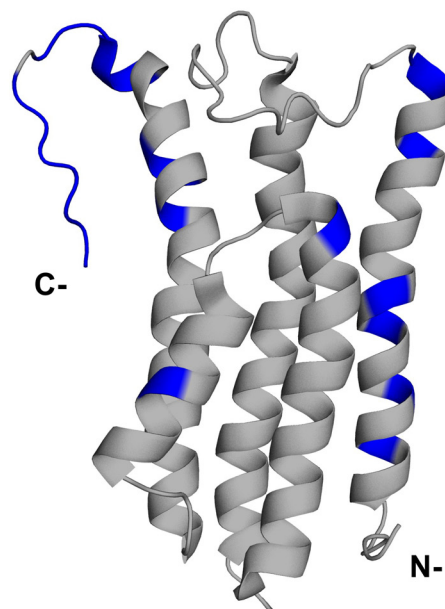| AA		Sequence	Peptide
1-18	B31	M I K C N N K T F N N L L K L T I L	A1
	297	M I K C N N K T F N N L L K L T I L	
19-36	B31	V N L L I S C G L T G A T K I R L E	A2
	297	V N L L I S C G L T G A T K I K L E	B9
28-45	B31	T G A T K I R L E R S A K D I T D E	A3
	297	T G A T K I K L E S S A K A I V D E	B10
37-54	B31	R S A K D I T D E I D A I K K D A A	A4
	297	S S A K A I V D E I D A I K K K A A	B11
46-63	B31	I D A I K K D A A L K G V N F D A F	A5
	297	I D A I K K A A S M G V N F D A F	B12
55-72	B31	L K G V N F D A F K D K K T G S G V	A6
	297	S M G V N F D A F K D K K T G S G V	C1
64-81	B31	K D K K T G S G V S E N P F I L E A	A7
	297	K D K K T G S G V S E N P F I L E A	
73-90	B31	S E N P F I L E A K V R A T T V A E	A8
	297	S E N P F I L E A K V R A T T V A E	
82-99	B31	K V R A T T V A E K F V I A I E E E	A9
	297	K V R A T T V A E K F V I A I E E E	
91-108	B31	K F V I A I E E E A T K L K E T G S	A10
	297	K F V I A I E E E A T K L K E T G S	
100-117	B31	A T K L K E T G S S G E F S A M Y D	A11
	297	A T K L K E T G S S G E F S A M Y D	
109-126	B31	S G E F S A M Y D L M F E V S K P L	A12
	297	S G E F S A M Y D L M F E V S K P L	
118-135	B31	L M F E V S K P L Q K L G I Q E M T	B1
	297	L M F E V S K P L Q E L G I Q E M T	C2
127-144	B31	Q K L G I Q E M T K T V S D A A E E	B2
	297	Q E L G I Q E M T K T V S M A A E E	C3
136-153	B31	K T V S D A A E E N P P T T A Q G V	B3
	297	K T V S M A A E E N P P T T A Q G V	C4
145-162	B31	N P P T T A Q G V L E I A K K M R E	B4
	297	N P P T T A Q G V L E I A K K M R E	
154-171	B31	L E I A K K M R E K L Q R V H T K N	B5
	297	L E I A K K M R E K L Q R V H K K N	C5
163-180	B31	K L Q R V H T K N Y C T L K K K E N	B6
	297	K L Q R V H K K N Q D T L K K K N T	C6
172-189	B31	Y C T L K K K E N S T F T D E K C K	B7
	297	Q D T L K K K N T E D S T A K S - -	C7
181-191	B31	S T F T D E K C K N N	B8

FIG 2 DbpA peptide arrays for *B. burgdorferi* strains B31 and 297. (A) Tabular alignment of DbpA amino acid number (left column), sequences (middle column), and corresponding peptide names for *B. burgdorferi* strains B31 (OspC Type A) and 297 (OspC Type K), as described in Materials and Methods. Residue differences between B31 and 297 are highlighted in purple in the table and are (B) illustrated using PyMol and PDB ID 2LQU on the structure of DbpA$_{B31}$. The final array contained 31 peptides: 8 that were identical between sequences, 12 that represented B31 sequences, and 11 that represented 297 sequences.

IgM$^+$/IgG$^+$ and IgM$^-$/IgG$^+$ cohorts, which is indicative of the maturation of the immune response with time (Fig. S1).

Reactivity of *B. burgdorferi*-seropositive serum samples with DbpA peptide array. To identify linear B cell epitopes on DbpA of *B. burgdorferi* strains B31 (DbpA$_{B31}$) and 297 (DbpA$_{297}$), we generated 18-mer peptide libraries that encompassed each of the DbpA variants. The DbpA amino acid sequences from *B. burgdorferi* strains B31 and 297 are 89% identical (16). As such, the final library consisted of a total of 31 peptides: 8 shared between strains B31 and 297, 12 specific to DbpA$_{B31}$, and 11 specific to DbpA$_{297}$ (Fig. 2).

To assess which (if any) DbpA-derived peptides are reactive with *B. burgdorferi*-seropositive sera, the peptides were coated onto 96-well microtiter plates and probed with control ($n = 4$) or seropositive ($n = 23$) human serum samples. IgM reactivity in the serum samples was limited to a few peptides, while IgG reactivity was much more pronounced, with ~60% of the peptides displaying above background reactivity (Fig. S2). Based on this cumulative reactivity profile by ELISA, a dozen DbpA peptides were chosen for detailed analysis by

Luminex with our larger *B. burgdorferi*-seropositive serum sample set. Included in our down-selection were peptides identified by the Bepipred linear epitope prediction tool as having a high likelihood of being a target of antibodies (e.g., residues spanning 55 to 78, 101 to 113, 126 to 136, and 165 to 187).

However, before performing the Luminex analysis, we examined antibody reactivity by ELISA with peptide A1 (DbpA residues 1 to 18) in more detail, as a peptide spanning residues 6 to 30 was recognized by sera from patients clinically diagnosed as having erythema migrans (EM), an early manifestation of Lyme disease (28). In our study, IgM and IgG reactivity with peptide A1 was 2- to 4-fold elevated over background, but this was only observed in a fraction (14 to 16%) of the samples tested (Fig. S3). Thus, our results are similar to those of Arnaboldi and colleagues in terms of IgM reactivity with peptide A1, but they differ in that we observed IgG reactivity with the same peptide. This discrepancy in IgG reactivity (low in the previous study, and detectable in our study) may simply be reflective of different patient populations, as one represented early-stage disease and the other a (two-tier positive) later stage. Overall, however, A1 antibody reactivity was considered low and was not included in the Luminex analysis.

Multiplex profiling of *B. burgdorferi*-seropositive serum reactivity with DbpA peptides. Based on peptide array profiling by ELISA, 12 highly reactive peptides were synthesized with an N-terminal linker (-GGGSK) and a biotin-tag, then coupled to streptavidin-coated Luminex beads. We then performed a multiplex analysis on samples from all three clinical cohorts (IgM$^+$/IgG$^-$, IgM$^+$/IgG$^+$, and IgM$^-$/IgG$^+$). We established a healthy cutoff value (MFI) using a commercial panel of 87 serum samples that displayed low IgM and IgG MFI values for DbpA as well as the 12 DbpA peptides (Table 1; Fig. 1).

The Luminex analysis revealed that all 12 DbpA-derived peptides were recognized by IgG from at least one of the three *B. burgdorferi*-seropositive cohorts (IgM$^+$/IgG$^-$, IgM$^+$/IgG$^+$, and IgM$^-$/IgG$^+$). With two exceptions (peptides A7 and C7, which will be discussed below), the increase in peptide reactivities ranged from 0.4- to 15-fold over those of healthy controls (Table 1). Nine of the 12 peptides were also recognized by IgM from at least one of the three *B. burgdorferi*-seropositive cohorts (IgM$^+$/IgG$^-$, IgM$^+$/IgG$^+$, and IgM$^-$/IgG$^+$) (Table S1). Except for peptides A7 and C7, the IgM reactivities with the peptides were only marginally above background.

DbpA-derived peptides A7 and C7 stood out as being highly reactive with IgG in the *B. burgdorferi*-seropositive serum panel (Table 1) and moderately reactive within the IgM pool (Table S1). Specifically, IgG reactivity with peptide A7, which corresponds to DbpA residues 64 to 81, was not significantly elevated in the IgM$^+$/IgG- serum panel, although it was 84-fold and 59-fold increased over background in the IgM$^+$/IgG$^+$ and IgM$^-$/IgG$^+$ sample sets, respectively (Table 1; Fig. 3). In the IgM fraction, A7 reactivity was significantly elevated (4- to 11-fold) in each of the three *B. burgdorferi*-seropositive cohorts (IgM$^+$/IgG$^-$, IgM$^+$/IgG$^+$, and IgM$^-$/IgG$^+$) (Table S1). The proximal peptide, corresponding to residues 55 to 72, was largely nonreactive for DbpA$_{B31}$ (peptide A6) and moderately reactive for DbpA$_{297}$ (peptide C1) (Table 1; Fig. 3). The reactivity of the distal flanking peptide (residues 73 to 90) was not examined by Luminex because the peptide (A8) was deemed nonreactive in our preliminary ELISA screen (Fig. S2) and was therefore not pursued further. Collectively, these results suggest that the A7 sequence constitutes an immunodominant epitope within itself.

The other notable peptide was C7, which corresponds to the extreme C-terminus of DbpA$_{297}$ (residues 172 to 187). While C7 reactivity was not significantly elevated in the IgM$^+$/IgG$^-$ serum panel, it was 84-fold and 58-fold increased over background in the IgM$^+$/IgG$^+$ and IgM$^-$/IgG$^+$ sample sets, respectively (Table 1; Fig. 4). In the IgM fraction, C7 reactivity was significantly elevated (3- to 5-fold) in each of the three *B. burgdorferi*-seropositive cohorts (IgM$^+$/IgG$^-$, IgM$^+$/IgG$^+$, and IgM$^-$/IgG$^+$) (Table S1). These results clearly demonstrate that the 16 C-terminal residues of DbpA$_{297}$ are targeted by antibodies in *B. burgdorferi*-seropositive samples.

However, we found it curious that the analogous C-terminal peptide (B7) from DbpA$_{B31}$ (residues 172 to 189) was only weakly reactive by Luminex, compared to peptide C7 from DbpA$_{297}$ (Fig. 4; Table S1), especially considering that B7 was one of the most reactive
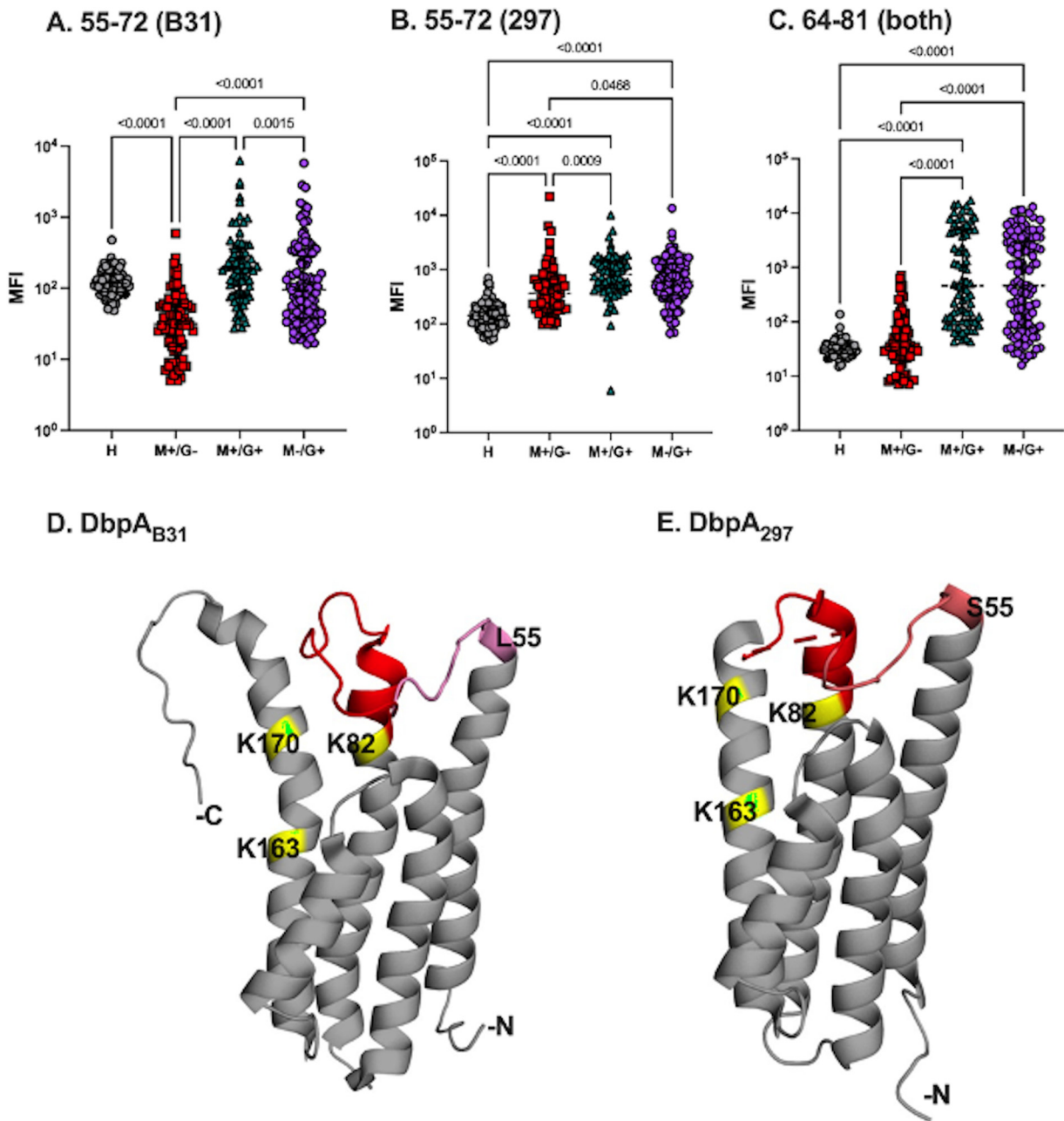
FIG 3 Reactivity of *B. burgdorferi*-seropositive serum samples with DbpA residues 55 to 81. IgG reactivity (MFI) in healthy (*n* = 86) or *B. burgdorferi*-seropositive serum samples defined as IgM⁺/IgG⁻ (*n* = 78), IgM⁺/IgG⁺ (*n* = 71), or IgM⁻/IgG⁺ (*n* = 114) for DbpA$_{B31}$ and DbpA$_{297}$ peptides spanning residues (A and B) 55 to 72 and (C) 64 to 81. Significance was determined by one-way ANOVA followed by Tukey's post hoc test. (D and E) PyMol images of DbpA$_{B31}$ (PDB ID 2LQU) and DbpA$_{297}$ (PDB ID 4ONR) with residues 64 to 81 are colored firebrick red, and residues 55 to 63 are colored in shades of pink, with darker shades representing greater reactivity. The three lysine residues implicated in decorin binding (K82, K163, and K170) are colored yellow/green.

peptides in our preliminary ELISA screen (Fig. S2). Moreover, B7 is predicted to have a high propensity to be a linear epitope, according to Bepipred. We reasoned that the subdued response to B7 by Luminex might simply be related to the nature of the multiplexed bead array itself, for reasons related to interference or surface coupling (35). We therefore performed a comprehensive analysis of 30 control (healthy) and ~270 *B. burgdorferi*-seropositive samples for peptide B7 reactivity by ELISA. Antibody reactivity with peptide B7 was significantly higher in *B. burgdorferi*-seropositive serum samples, compared to that of
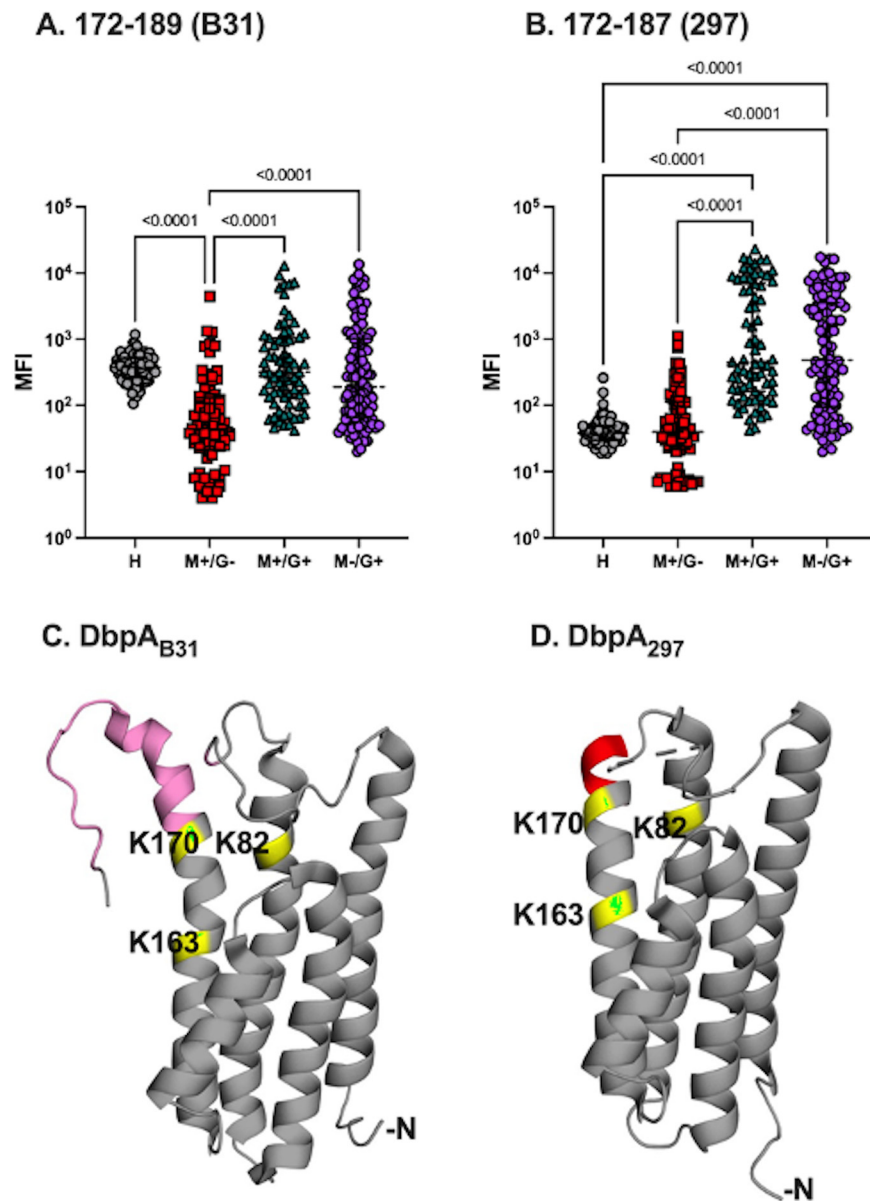
FIG 4 Reactivity of *B. burgdorferi*-seropositive serum samples with DbpA C-terminal residues. IgG reactivity (MFI) in healthy ($n = 86$), or *B. burgdorferi*-seropositive serum samples defined as IgM+/IgG− ($n = 78$), IgM+/IgG+ ($n = 71$), IgM−/IgG+ ($n = 114$) for (A) DbpA$_{B31}$ residues 172 to 189 and (B) DbpA$_{297}$ residues 172 to 187. Significance was determined by one-way ANOVA followed by Tukey's *post hoc* tests. PyMol images of (C) DbpA$_{B31}$ (PDB ID 2LQU) with residues 172 to 189 colored pink and DbpA$_{297}$ (PDB ID 4ONR) with residues 172 to 187 colored firebrick red. Residues 172 to 187 in DbpA$_{297}$ are disordered and not visible in 4ONR. The three lysine residues implicated in decorin binding (K82, K163 and K170) are colored yellow/green.

healthy controls ($P < 0.001$) (Fig. S4), thereby confirming our earlier observation that the C-terminus (residues 172 to 189) of DbpA$_{B31}$ constitutes an immunodominant linear epitope.

Relationship between DbpA and peptide reactivity. To determine whether reactivity to a particular peptide was simply proportional to overall DbpA antibody titers in any given individual, we determined the correlation coefficients between the DbpA MFI values and the peptide MFI values for each of the $\sim$270 serum samples. As shown in Fig. S5, there was no notable correlation between the two variables, except for peptide A7, which had an R^2 value approaching 0.4, indicating a weak to moderate relationship between DbpA and
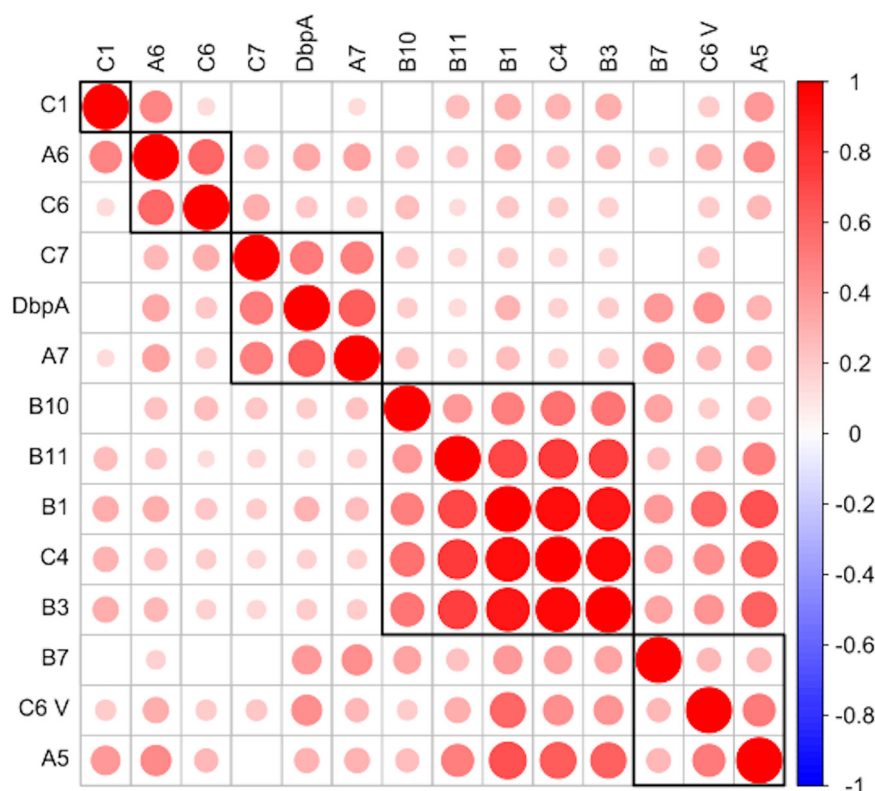
FIG 5 Correlation matrix of antibody responses to specific DbpA peptides. Pearson correlations were calculated for every possible combination of DbpA and peptide from the values presented in Table 1, and the resulting *P* values were adjusted for multiple comparisons by the Benjamini-Hochberg method. Correlations with significant adjusted *P* values are displayed in the matrices, while those with insignificant *P* values are left blank. The color (per scale on right) and relative size of each dot correspond to the strength of the corresponding correlation, and black rectangles around groups of correlations show the results of hierarchical clustering of the peptides.

peptide-specific antibody levels. This observation raises the possibility that anti-peptide antibodies are elicited against DbpA breakdown products rather than intact (native) DbpA.

To better assess the relationship between DbpA and peptide recognition, we examined correlations between available MFIs for all serum samples. A correlation matrix of serum IgG samples revealed four sets of peptides whose reactivity profiles tracked with each other, even though the peptides were not necessarily overlapping or even on adjacent regions of DbpA (Fig. 5). For example, the reactivities of A6 and C6 correlated with each other, as did those of C7, A7, and DbpA. The largest cluster consisted of B10, B11, B1, C4, and B3, which represent overlapping peptides (B10, B11), abutting peptides (B1, B3), and a solitary peptide (C4). The same correlations did not hold when IgM reactivity was examined, primarily because of much higher background values, which confounded our ability to sort out specific versus nonspecific relationships (data not shown). From this analysis, the correlation between the C7, A7, and DbpA reactivities was the most compelling, as those two peptides were identified as being highly reactive in the serum panel examined (Table 1).

Native versus non-native linear B cell epitopes on DbpA. The elicitation of antibodies against linear epitopes on a given protein antigen can occur in the context of the antigen's native conformation (e.g., by being displayed on the surface of the pathogen) or non-native conformation, induced upon antigen release and/or degradation from the pathogen (36). In an effort to distinguish between these two categories in the case of DbpA, we reprobed four different peptide-coated microspheres in the absence and presence of a soluble recombinant DbpA (10 μg/mL) competitor. We reasoned that the reactivity of human antisera with a native linear epitope would compete with soluble recombinant
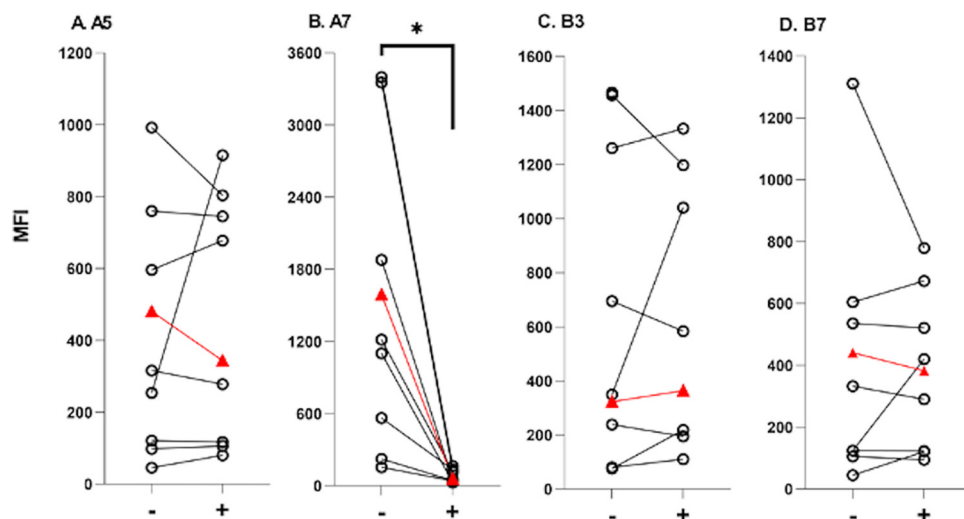
FIG 6 Recognition of recombinant DbpA by peptide-specific antibodies. *B. burgdorferi*-seropositive serum samples were incubated without (−) and with (+) soluble DbpA (10 μg/mL), then mixed with four different peptide-coated bead sets, as indicated in Panels A–D, and subjected to Luminex analysis. The relative reactivities (MFI; *y*-axis) without and with DbpA are plotted with individual samples connected by a line. Included in the analysis is an Accurun (+) sample indicated by the triangle (red). Only the reactivity of peptide A7 was reduced by the addition of soluble DbpA, as reflected by a reduction in MFI in the (+) column compared to the (−) column. Significance was determined by paired, two-tailed *t*-tests with Welch's corrections. *, $P \leq 0.05$.

DbpA, whereas reactivity to cryptic or non-native linear epitopes would not. Analysis of a subset of human serum samples revealed an immediate trend. Specifically, the addition of soluble DbpA had little or no inhibitory effect on antisera reactivity with A5, B3, and B7-coated beads (Fig. 6). Peptides B11 and C7 served as controls for these studies, as competition was not expected from them in the first place, since these peptides are derived from the *B. burgdorferi* strain 297 sequence and are sufficiently divergent from the DbpA$_{B31}$ sequence (data not shown). Peptide A7 was different in that antibody reactivity was uniformly eliminated upon the addition of soluble DbpA in the *B. burgdorferi*-seropositive serum samples tested. We interpret these results as an indication that peptide A7 (residues 64 to 81) constitutes a surface exposed linear B cell epitope on DbpA, while epitopes A5 and B3 are cryptic in nature, with the caveat that we cannot fully exclude the possibility that the recombinant DbpA used for the competition studies does not necessarily reflect the native antigen when displayed on the spirochete surface.

DISCUSSION

DbpA is one of the most antigenic outer surface proteins of *B. burgdorferi*, and, as such, has important implications for LD diagnostics and immunity (13, 14, 34, 37, 38). Indeed, antibodies against DbpA have been shown to promote the resolution of early *B. burgdorferi* infections (11). However, despite DbpA's importance as an immune target, little is known about the specific epitopes on DbpA that are recognized by humans. To begin to address this question, we profiled a collection of ~270 archived human *B. burgdorferi*-seropositive serum samples for reactivity with a DbpA peptide array derived from two geographically representative *B. burgdorferi* type strains, B31 (OspC Type A) and 297 (OspC Type K). Twelve of the original 31 peptides reactive by ELISA were resynthesized with biotin-tags to enable multiplex analysis against the full suite of healthy and *B. burgdorferi*-seropositive sera (IgM⁺/IgG⁻, IgM⁺/IgG⁺, and IgM⁻/IgG⁺) in our collection. While the results revealed significant IgG (and some IgM) reactivity against essentially all of the peptides examined, two stretches of DbpA stood out as being highly immunoreactive, defined as displaying a >20-fold increase over the reactivity observed in healthy controls. The first stretch corresponds to DbpA residues 64 to 81 (peptide A7), an amino acid sequence conserved between DbpA$_{B31}$ and DbpA$_{297}$. The second corresponds

to the respective C-terminal peptides of DbpA$_{B31}$ (B7; residues 172 to 189) and DbpA$_{297}$ (C7; residues 172 to 187), which are notably divergent from each other. Identification of these linear epitopes on DbpA may have utility in both Lyme disease diagnostics and, potentially, a next-generation Lyme disease vaccine.

DbpA residues 64 to 81 (peptide A7) are conserved between *B. burgdorferi* strains B31 and 297. When mapped onto the solution structure of DbpA$_{B31}$ (PDB ID 2LQU), as shown in Fig. 3, the A7 peptide corresponds to the flexible loop between DbpA's α-helix 1 and α-helix 2 in proximity to three key lysine residues (K82, K163, and K170) associated with heparin and decorin binding (16, 19). The peptide is similarly positioned on DbpA$_{297}$, although the actual loop is disordered in the DbpA$_{297}$ crystal structure (PDB ID 4ONR). In the case of DbpA$_{B31}$, the two flanking peptides (A6 and A8) were only mildly reactive in our arrays, as was the flanking C1 peptide (residues 55 to 72) for DbpA$_{297}$, suggesting that the central loop itself, rather than the adjacent α-helices, is the most immunoreactive. Interestingly, Tokarz and colleagues identified this same region as being reactive with antisera from patients with Lyme neuroborreliosis (IEDB ID 745110) (29). Thus, we propose that the flexible loop between α-helix 1 and α-helix 2 (and certain flanking residues) constitutes an immunodominant linear epitope on DbpA that is recognized in *B. burgdorferi*-seropositive patients and possibly in LD. Indeed, the same loop and flanking regions are predicted to contain conformational B cell epitopes, according to Discotope (39) and ElliPro (40). Finally, it is also noteworthy that the A7 peptide contains a tripartite motif (Thr-Gly-Ser) that is conserved in DbpA and DbpB from *B. burgdorferi* and *B. garinii*, although the functional significance of this motif is unknown (41).

The flexible linker between α-helix 1 and α-helix 2 has been implicated in influencing DbpA's affinity for GAGs, raising the possibility that antibodies directed against the A7 peptide epitope block the interaction of DbpA and substrate (42–44). In the case of DbpA from *B. burgdorferi* strain N40, shortening the linker via the deletion of residues 62 to 71 resulted in DbpA having a ~2-fold increased affinity for heparin and dematan sulfate, an observation that is consistent with the loop physically occluding the GAG binding pocket (43). Hook and colleagues have argued that DbpA$_{B31}$ and DbpA$_{297}$ residues 76 to 90 (corresponding to peptides A7 and A8 in our array) contain a decorin binding site of their own. Specifically, they reported that a soluble peptide encompassing residues 76 to 90 (PFILEAKVRATTVAE) was sufficient to competitively inhibit biotin-labeled DbpA from adhering to immobilized decorin (45). In addition, antiserum raised against this peptide reduced DbpA-decorin binding by ~50%. Collectively, these results argue that human antibodies directed against peptide A7 would partially, if not completely, inhibit DbpA attachment to the ECM. Those same A7-specific antibodies would also presumably promote complement-mediated borreliacidal activity (6, 18, 27, 46). We are actively pursuing these hypotheses and have already demonstrated that the immunization of mice with an A7-KLH conjugate gives rise to DbpA-specific antibodies, confirming that residues 64-87 constitute a native linear epitope on DbpA. (E. Movahed and N. Mantis, unpublished results).

Peptides B7 (residues 172 to 189) and C7 (residues 172 to 187) from DbpA$_{B31}$ and DbpA$_{297}$, respectively, are also potentially consequential antibody targets, considering that the C-terminus of DbpA has been proposed to contribute to attachment to GAGs (15). Specifically, the C-terminal residues of DbpA are lysine-rich, with DbpA$_{B31}$ and DbpA$_{297}$ sharing a common KKK core motif (residues 176 to 178). Benoit and colleagues demonstrated that DbpA truncations were properly displayed on the spirochete outer surface but that resulting strains were unable to attach to 293 cells or immobilized GAGs (15). The available structures suggest that the DbpA's C-terminus projects away from the bacterial surface and is readily accessible to substrates (and antibodies). In our study, peptide C7 was highly reactive with *B. burgdorferi*-seropositive serum, as measured by Luminex and ELISA, whereas the B7 peptide was reactive by ELISA but not Luminex. It is unclear whether the difference in B7 reactivity is due to the surface charge associated with polystyrene beads versus polystyrene Maxisorb ELISA plates or whether the biotin-tagged B7 peptide used for Luminex assumes a conformation not conducive to antibody

recognition. Sorting this issue out has obvious implications, should B7 and other similar peptides be used as possible diagnostic markers for serology (37, 47).

In conclusion, this study represents an early effort to begin to better understand the human antibody response to DbpA and the role anti-DbpA antibodies play in resolving infection (48, 49). Certainly, the immunogenic nature of DbpA alone is of interest in terms of defining which pathogen-associated proteins stimulate B cell activation in humans and why this occurs (48, 49). DbpA is similarly immunoreactive in experimentally-infected Rhesus macaques and other species (12). In mice, for example, DbpA has been shown to be a T cell-independent antigen, indicating that it has the capacity to activate B cells directly in the absence of CD4 T helper cells (26). Whether this also applies to humans and/or contributes to the antigenicity of DbpA remains an open question. It is also unclear to what degree antibodies are elicited to native DbpA, as displayed on the bacterial surface, or to conformations of DbpA that may arise following bacterial lysis and protein release (50).

MATERIALS AND METHODS

Chemicals and biological reagents. Chemicals and reagents were obtained from Thermo Fisher, Inc. (Waltham, MA), unless noted otherwise. PBS was prepared by the Wadsworth Center's Cell and Tissue culture core facility.

Cloning, expression, and purification of recombinant DbpA. DbpA from *B. burgdorferi* B31 (NCBI: txid224326) was expressed in *E. coli* BL21 (DE3). The PCR amplicons for DbpA residues 26 to 188 were subcloned into the pNYCOMPS-C-term expression vector, encoding a C-terminal deca-His tag. The transformed *E. coli* BL21 (DE3) strain was grown at 37°C in TB medium until mid-log-phase (0.6 at OD_{600}), after which it was treated with 0.1 mM IPTG and cultured for 16 h at 20°C. The cells were harvested by centrifugation and resuspended in 20 mM Tris-Cl (pH 7.5) and 150 mM NaCl. The cell suspension was sonicated and centrifuged at 30,000 × g for 30 min. After centrifugation, the protein-containing supernatant was purified by nickel-affinity and size exclusion chromatography on an AKTAxpress system (GE Healthcare), which consisted of a 1 mL nickel affinity column followed by a Superdex 200 16/60 gel filtration column. The elution buffer consisted of 0.5 M imidazole in binding buffer, and the gel filtration buffer consisted of 20 mM HEPES pH 7.6, 150 mM NaCl, and 20 mM imidazole. Fractions containing pure DbpA were pooled and subjected to TEV protease cleavage (1:10 weight ratio) for 3 h at room temperature to remove the deca-His tag. The cleaved protein was passed over a 1 mL Ni-NTA agarose (Qiagen) gravity column to remove the TEV protease, deca-histidine tag, and any uncleaved protein. DpbA was then buffer exchanged into 20 mM HEPES (pH 7.5) and 150 mM NaCl.

Prediction of DbpA linear B cell epitopes. The sequence of DbpA from *B. burgdorferi* strains B31 (DbpA$_{B31}$; UniProt ID O50917) and 297 (DbpA$_{297}$; UniProt ID Q1W5I8) were analyzed using the linear B cell epitope prediction tool Bepipred (set threshold 0.5) (30), available via the Immune Epitope Database (IEDB.org) (31).

DbpA peptide array. The DbpA sequences from *B. burgdorferi* strains B31 (OspC Type A; NCBI: txid224326) and 297 (OspC Type K; NCBI: txid521009) are ~89% identical. Peptide arrays covering DbpA from *B. burgdorferi* strains B31 and 297 were designed based on NCBI taxonomy ID sequences, as noted above, and synthesized by NeoScientific (Woburn, MA). The final library consisted of 31 peptides, of which 8 were identical between sequences, 12 were specific to B31, and 11 were specific to 297 (presented in Fig. 2). Each peptide was 18 amino acids in length and overlapped with the previous peptide by 9 residues, with the omission of a single peptide corresponding to residues 10 to 27, which failed Q/C. The peptides were solubilized in dimethyl sulfoxide (DMSO) at 10 mg/mL, and aliquots were stored at −20°C. Aliquots were thawed as needed and diluted in PBS (1 to 10 μg/mL) for routine use. Of the 31 original peptides, 12 that were reactive with a subset of *B. burgdorferi*-seropositive samples were ordered with a C-terminal GGGSK extension that was biotinylated on the terminal lysine (Genemed Synthesis, San Francisco, CA).

Commercial and *B. burgdorferi*-seropositive serum samples. Commercial Lyme disease seronegative (Lot 10500586) and seropositive (Lot 10510438) pooled samples were used as controls throughout this study (ACCURUN 810 and 130, respectively; SeraCare, Milford, MA). Healthy controls consisted of a commercial panel of 87 serum samples collected in 2017 and 2018 (Access Biologicals, Vista, CA). Primary clinical samples were obtained from the Wadsworth Center's Diagnostic Immunology Laboratory. Those samples were submitted for Lyme disease serology and subjected to two-tiered testing consisting of (Tier 1) a C6 peptide screen (Immunetics; C6 Lyme ELISA) or Enzyme Linked Fluorescent Assay (ELFA; bioMérieux, VIDAS Lyme IgG II, and Lyme IgM II; Durham, NC) followed by (Tier 2) IgM and IgG detection by Western blotting (MarDX; Trinity Biotech, Carlsbad, CA). *B. burgdorferi*-specific IgM reactivity was defined as ≥2 positive bands, with IgG reactivity defined as ≥5 positive bands. Serum samples were aliquoted, de-identified, and classified as IgM-positive/IgG-negative, IgM-positive/IgG-positive, or IgM-negative/IgG-positive, based on the Western blot results. For this study, we employed a total of ~270 serum samples.

ELISA and preliminary pepscan analysis. Nunc Maxisorb F96 microtiter plates (Thermo Fisher Scientific) were coated with DbpA (0.1 μg/well) or DbpA peptides (1.0 μg/well) in PBS (pH 7.4), then incubated overnight at 4°C. The plates were washed three times with PBS-Tween 20 (PBS-T; 0.1%, vol/vol) and blocked with goat serum (2%, vol/vol, in PBS-T) for 2 h at room temperature before being

probed with serum samples (1:100 dilution). Plate bound antibodies were detected with horseradish peroxidase (HRP)-labeled goat anti-human IgG or IgM polyclonal antibodies (SouthernBiotech, Birmingham, AL). The plates were developed with 3,3, 5,5-tetramethylbenzidine (TMB; Kirkegaard & Perry Labs, Gaithersburg, MD) and analyzed using a SpectroMax 250 spectrophotometer (Molecular Devices, Sunnyvale, CA).

Multiplexed DbpA and peptide microsphere immunoassays (MIA). Recombinant DbpA (5 μg) was coupled to Magplex-C microspheres (1 $\times$ 10^6) using sulfo-NHS (N-hydroxysulfosuccinimide) and EDC (1-ethyl-3-[3-dimethylaminopropyl] carbodiimide hydrochloride), as recommended by the manufacturer (Luminex Corp., Austin, TX). Coupled beads were diluted in storage buffer (phosphate-buffered saline [PBS] with 1% bovine serum albumin [BSA], 0.02% Tween 20, 0.05% azide, pH 7.4) to a concentration of 1 $\times$ 10^6 beads/mL.

Biotin-labeled peptides were complexed to Megaplex-avidin microspheres, following protocols provided by the manufacturer (Luminex Corp.). Briefly, microspheres were washed and resuspended in 250 μL of PBS-BSA, then subjected to vortexing and sonication. A total of 1.0 $\times$ 10^6 beads in PBS-BSA were mixed with biotin-conjugated DbpA peptides ($\sim$5 μg) and incubated for 30 min at room temperature. The microsphere suspensions were then washed three times using a magnetic separator, resuspended in 500 μL of storage buffer, and stored at 4°C until use. Samples were analyzed using a FlexMap 3D instrument (Luminex Corp.).

Statistical analysis. ANOVAs and Student's *t*-tests were carried out using GraphPad Prism, V 9.1 (Systat Software, San Jose, CA). Correlation matrices were prepared to examine correlations between MFI values of all responses to peptides, separated into IgG and IgM responses, using the R package corrplot (51).

Molecular modeling. The open-source molecular visualization software PyMol (DeLano Scientific LLC, Palo Alto, CA) was accessed at www.pymol.org and used for epitope modeling. Modeling was performed using DbpA structures PDB ID 4ONR (strain 297) and 2LQU (strain B31), available from the Protein Data Bank (rcsb.org) (19, 52).

SUPPLEMENTAL MATERIAL

Supplemental material is available online only.

FIG S1, TIF file, 1.9 MB.
FIG S2, TIF file, 1.9 MB.
FIG S3, TIF file, 1.9 MB.
FIG S4, TIF file, 1.9 MB.
FIG S5, TIF file, 1.9 MB.
TABLE S1, DOCX file, 0.02 MB.

REFERENCES

1. Steere AC, Strle F, Wormser GP, Hu LT, Branda JA, Hovius JW, Li X, Mead PS. 2016. Lyme borreliosis. Nat Rev Dis Primers 2:16090. https://doi.org/10.1038/nrdp.2016.90.

2. Brandt KS, Ullmann AJ, Molins CR, Horiuchi K, Biggerstaff BJ, Gilmore RD. 2019. Evaluation of in vivo expressed Borrelia burgdorferi antigens for improved IgM serodiagnosis of early Lyme disease. Diagn Microbiol Infect Dis 93:196–202. https://doi.org/10.1016/j.diagmicrobio.2018.09.012.

3. Lantos PM, Rumbaugh J, Bockenstedt LK, Falck-Ytter YT, Aguero-Rosenfeld ME, Auwaerter PG, Baldwin K, Bannuru RR, Belani KK, Bowie WR, Branda JA, Clifford DB, DiMario FJ, Halperin JJ, Krause PJ, Lavergne V, Liang MH, Meissner HC, Nigrovic LE, Nocton JJJ, Osani MC, Pruitt AA, Rips J, Rosenfeld LE, Savoy ML, Sood SK, Steere AC, Strle F, Sundel R, Tsao J, Vaysbrot EE, Wormser GP, Zemel LS. 2021. Clinical practice guidelines by the Infectious Diseases Society of America (IDSA), American Academy of Neurology (AAN), and American College of Rheumatology (ACR): 2020 guidelines for the prevention, diagnosis and treatment of Lyme disease. Clin Infect Dis 72:1–8. https://doi.org/10.1093/cid/ciaa1215.

4. Molins CR, Delorey MJ, Sexton C, Schriefer ME. 2016. Lyme Borreliosis serology: performance of several commonly used laboratory diagnostic tests and a large resource panel of well-characterized patient samples. J Clin Microbiol 54:2726–2734. https://doi.org/10.1128/JCM.00874-16.

5. Kochi SK, Johnson RC. 1988. Role of immunoglobulin G in killing of Borrelia burgdorferi by the classical complement pathway. Infect Immun 56:314–321. https://doi.org/10.1128/iai.56.2.314-321.1988.

6. LaRocca TJ, Benach JL. 2008. The important and diverse roles of antibodies in the host response to Borrelia infections. Curr Top Microbiol Immunol 319:63–103. https://doi.org/10.1007/978-3-540-73900-5_4.

7. Zhi H, Xie J, Skare JT. 2018. The classical complement pathway is required to control Borrelia burgdorferi levels during experimental infection. Front Immunol 9:959. https://doi.org/10.3389/fimmu.2018.00959.

8. Benach JL, Fleit HB, Habicht GS, Coleman JL, Bosler EM, Lane BP. 1984. Interactions of phagocytes with the Lyme disease spirochete: role of the Fc receptor. J Infect Dis 150:497–507. https://doi.org/10.1093/infdis/150.4.497.

9. Benjamin SJ, Hawley KL, Vera-Licona P, La Vake CJ, Cervantes JL, Ruan Y, Radolf JD, Salazar JC. 2021. Macrophage mediated recognition and clearance of Borrelia burgdorferi elicits MyD88-dependent and -independent phagosomal signals that contribute to phagocytosis and inflammation. BMC Immunol 22:32. https://doi.org/10.1186/s12865-021-00418-8.

10. Feng S, Hodzic E, Stevenson B, Barthold SW. 1998. Humoral immunity to Borrelia burgdorferi N40 decorin binding proteins during infection of laboratory mice. Infect Immun 66:2827–2835. https://doi.org/10.1128/IAI.66.6.2827-2835.1998.

11. Hanson MS, Cassatt DR, Guo BP, Patel NK, McCarthy MP, Dorward DW, Hook M. 1998. Active and passive immunity against Borrelia burgdorferi decorin binding protein A (DbpA) protects against infection. Infect Immun 66:2143–2153. https://doi.org/10.1128/IAI.66.5.2143-2153.1998.

12. Embers ME, Hasenkampf NR, Jacobs MB, Philipp MT. 2012. Dynamic longitudinal antibody responses during Borrelia burgdorferi infection and antibiotic treatment of rhesus macaques. Clin Vaccine Immunol 19:1218–1226. https://doi.org/10.1128/CVI.00228-12.

13. Xu Y, Bruno JF, Luft BJ. 2008. Profiling the humoral immune response to Borrelia burgdorferi infection with protein microarrays. Microb Pathog 45:403–407. https://doi.org/10.1016/j.micpath.2008.09.006.

14. Embers ME, Hasenkampf NR, Barnes MB, Didier ES, Philipp MT, Tardo AC. 2016. Five-antigen fluorescent bead-based assay for diagnosis of Lyme disease. Clin Vaccine Immunol 23:294–303. https://doi.org/10.1128/CVI.00685-15.

15. Benoit VM, Fischer JR, Lin YP, Parveen N, Leong JM. 2011. Allelic variation of the Lyme disease spirochete adhesin DbpA influences spirochetal binding to decorin, dermatan sulfate, and mammalian cells. Infect Immun 79:3501–3509. https://doi.org/10.1128/IAI.00163-11.

16. Brown EL, Guo BP, O'Neal P, Höök M. 1999. Adherence of Borrelia burgdorferi. identification of critical lysine residues in DbpA required for decorin binding. J Biol Chem 274:26272–26278. https://doi.org/10.1074/jbc.274.37.26272.

17. Caine JA, Coburn J. 2016. Multifunctional and redundant roles of Borrelia burgdorferi outer surface proteins in tissue adhesion, colonization, and complement evasion. Front Immunol 7:442. https://doi.org/10.3389/fimmu.2016.00442.

18. Cassatt DR, Patel NK, Ulbrandt ND, Hanson MS. 1998. DbpA, but not OspA, is expressed by Borrelia burgdorferi during spirochetemia and is a target for protective antibodies. Infect Immun 66:5379–5387. https://doi.org/10.1128/IAI.66.11.5379-5387.1998.

19. Fortune DE, Lin YP, Deka RK, Groshong AM, Moore BP, Hagman KE, Leong JM, Tomchick DR, Blevins JS. 2014. Identification of lysine residues in the Borrelia burgdorferi DbpA adhesin required for murine infection. Infect Immun 82:3186–3198. https://doi.org/10.1128/IAI.02036-14.

20. Guo BP, Brown EL, Dorward DW, Rosenberg LC, Hook M. 1998. Decorin-binding adhesins from Borrelia burgdorferi. Mol Microbiol 30:711–723. https://doi.org/10.1046/j.1365-2958.1998.01103.x.

21. Hyde JA, Trzeciakowski JP, Skare JT. 2007. Borrelia burgdorferi alters its gene expression and antigenic profile in response to CO2 levels. J Bacteriol 189:437–445. https://doi.org/10.1128/JB.01109-06.

22. Lin YP, Benoit V, Yang X, Martinez-Herranz R, Pal U, Leong JM. 2014. Strain-specific variation of the decorin-binding adhesin DbpA influences the tissue tropism of the lyme disease spirochete. PLoS Pathog 10:e1004238. https://doi.org/10.1371/journal.ppat.1004238.

23. Ojaimi C, Brooks C, Casjens S, Rosa P, Elias A, Barbour A, Jasinskas A, Benach J, Katona L, Radolf J, Caimano M, Skare J, Swingle K, Akins D, Schwartz I. 2003. Profiling of temperature-induced changes in Borrelia burgdorferi gene expression by using whole genome arrays. Infect Immun 71:1689–1705. https://doi.org/10.1128/IAI.71.4.1689-1705.2003.

24. Wang X. 2012. Solution structure of decorin-binding protein A from Borrelia burgdorferi. Biochemistry 51:8353–8362. https://doi.org/10.1021/bi3007093.

25. Brown EL, Wooten RM, Johnson BJ, Iozzo RV, Smith A, Dolan MC, Guo BP, Weis JJ, Höök M. 2001. Resistance to Lyme disease in decorin-deficient mice. J Clin Invest 107:845–852. https://doi.org/10.1172/JCI11692.

26. Elsner RA, Hastey CJ, Olsen KJ, Baumgarth N. 2015. Suppression of long-lived humoral immunity following Borrelia burgdorferi infection. PLoS Pathog 11:e1004976. https://doi.org/10.1371/journal.ppat.1004976.

27. Hagman KE, Yang X, Wikel SK, Schoeler GB, Caimano MJ, Radolf JD, Norgard MV. 2000. Decorin-binding protein A (DbpA) of Borrelia burgdorferi is not protective when immunized mice are challenged via tick infestation and correlates with the lack of DbpA expression by B. burgdorferi in ticks. Infect Immun 68:4759–4764. https://doi.org/10.1128/IAI.68.8.4759-4764.2000.

28. Arnaboldi PM, Sambir M, Dattwyler RJ. 2014. Decorin binding proteins A and B in the serodiagnosis of Lyme disease in North America. Clin Vaccine Immunol 21:1426–1436. https://doi.org/10.1128/CVI.00383-14.

29. Tokarz R, Mishra N, Tagliafierro T, Sameroff S, Caciula A, Chauhan L, Patel J, Sullivan E, Gucwa A, Fallon B, Golightly M, Molins C, Schriefer M, Marques A, Briese T, Lipkin WI. 2018. A multiplex serologic platform for diagnosis of tick-borne diseases. Sci Rep 8:3158. https://doi.org/10.1038/s41598-018-21349-2.

30. Larsen JE, Lund O, Nielsen M. 2006. Improved method for predicting linear B-cell epitopes. Immunome Res 2:2. https://doi.org/10.1186/1745-7580-2-2.

31. Vita R, Overton JA, Greenbaum JA, Ponomarenko J, Clark JD, Cantrell JR, Wheeler DK, Gabbard JL, Hix D, Sette A, Peters B. 2015. The immune epitope database (IEDB) 3.0. Nucleic Acids Res 43:D405–D412. https://doi.org/10.1093/nar/gku938.

32. Baum E, Randall AZ, Zeller M, Barbour AG. 2013. Inferring epitopes of a polymorphic antigen amidst broadly cross-reactive antibodies using protein microarrays: a study of OspC proteins of Borrelia burgdorferi. PLoS One 8:e67445. https://doi.org/10.1371/journal.pone.0067445.

33. Goettner G, Schulte-Spechtel U, Hillermann R, Liegl G, Wilske B, Fingerle V. 2005. Improvement of Lyme borreliosis serodiagnosis by a newly developed recombinant immunoglobulin G (IgG) and IgM line immunoblot assay and addition of VlsE and DbpA homologues. J Clin Microbiol 43:3602–3609. https://doi.org/10.1128/JCM.43.8.3602-3609.2005.

34. Schulte-Spechtel U, Fingerle V, Goettner G, Rogge S, Wilske B. 2006. Molecular analysis of decorin-binding protein A (DbpA) reveals five major groups among European Borrelia burgdorferi sensu lato strains with impact for the development of serological assays and indicates lateral gene transfer of the dbpA gene. Int J Med Microbiol 296 Suppl 40:250–266. https://doi.org/10.1016/j.ijmm.2006.01.006.

35. Elshal MF, McCoy JP. 2006. Multiplex bead array assays: performance evaluation and comparison of sensitivity to ELISA. Methods 38:317–323. https://doi.org/10.1016/j.ymeth.2005.11.010.

36. Cirelli KM, Crotty S. 2017. Germinal center enhancement by extended antigen availability. Curr Opin Immunol 47:64–69. https://doi.org/10.1016/j.coi.2017.06.008.

37. Bradshaw GL, Thueson RK, Uriona TJ. 2017. Improved serodiagnostic performance for Lyme disease by use of two recombinant proteins in enzyme-linked immunosorbent assay compared to standardized two-tier testing. J Clin Microbiol 55:3046–3056. https://doi.org/10.1128/JCM.01004-17.

38. Cinco M, Ruscio M, Rapagna F. 2000. Evidence of Dbps (decorin binding proteins) among European strains of Borrelia burgdorferi sensu lato and in the immune response of LB patient sera. FEMS Microbiol Lett 183:111–114. https://doi.org/10.1111/j.1574-6968.2000.tb08942.x.

39. Kringelum JV, Lundegaard C, Lund O, Nielsen M. 2012. Reliable B cell epitope predictions: impacts of method development and improved benchmarking. PLoS Comput Biol 8:e1002829. https://doi.org/10.1371/journal.pcbi.1002829.

40. Ponomarenko J, Bui HH, Li W, Fusseder N, Bourne PE, Sette A, Peters B. 2008. ElliPro: a new structure-based tool for the prediction of antibody epitopes. BMC Bioinformatics 9:514. https://doi.org/10.1186/1471-2105-9-514.

41. Pietikainen A, Astrand M, Cuellar J, Glader O, Elovaara H, Rouhiainen M, Salo J, Furihata T, Salminen TA, Hytonen J. 2021. Conserved lysine residues in decorin binding proteins of Borrelia garinii are critical in adhesion to human brain microvascular endothelial cells. Mol Microbiol 115:1395–1409. https://doi.org/10.1111/mmi.14687.

42. Morgan A, Wang X. 2013. The novel heparin-binding motif in decorin-binding protein A from strain B31 of Borrelia burgdorferi explains the higher binding affinity. Biochemistry 52:8237–8245. https://doi.org/10.1021/bi401376u.

43. Morgan A, Sepuru KM, Feng W, Rajarathnam K, Wang X. 2015. Flexible linker modulates glycosaminoglycan affinity of decorin binding protein A. Biochemistry 54:5113–5119. https://doi.org/10.1021/acs.biochem.5b00253.

44. Morgan AM, Wang X. 2015. Structural mechanisms underlying sequence-dependent variations in GAG affinities of decorin binding protein A, a Borrelia burgdorferi adhesin. Biochem J 467:439–451. https://doi.org/10.1042/BJ20141201.

45. Pikas DS, Brown EL, Gurusiddappa S, Lee LY, Xu Y, Hook M. 2003. Decorin-binding sites in the adhesin DbpA from Borrelia burgdorferi: a synthetic peptide approach. J Biol Chem 278:30920–30926. https://doi.org/10.1074/jbc.M303979200.

46. Ulbrandt ND, Cassatt DR, Patel NK, Roberts WC, Bachy CM, Fazenbaker CA, Hanson MS. 2001. Conformational nature of the Borrelia burgdorferi decorin binding protein A epitopes that elicit protective antibodies. Infect Immun 69:4799–4807. https://doi.org/10.1128/IAI.69.8.4799-4807.2001.

47. Pflughoeft KJ, Mash M, Hasenkampf NR, Jacobs MB, Tardo AC, Magee DM, Song L, LaBaer J, Philipp MT, Embers ME, AuCoin DP. 2019. Multi-platform approach for microbial biomarker identification using Borrelia burgdorferi as a model. Front Cell Infect Microbiol 9:179. https://doi.org/10.3389/fcimb.2019.00179.

48. McKisic MD, Barthold SW. 2000. T-cell-independent responses to Borrelia burgdorferi are critical for protective immunity and resolution of lyme disease. Infect Immun 68:5190–5197. https://doi.org/10.1128/IAI.68.9.5190-5197.2000.

49. Bobe JR, Jutras BL, Horn EJ, Embers ME, Bailey A, Moritz RL, Zhang Y, Soloski MJ, Ostfeld RS, Marconi RT, Aucott J, Ma'ayan A, Keesing F, Lewis K, Ben Mamoun C, Rebman AW, McClune ME, Breitschwerdt EB, Reddy PJ, Maggi R, Yang F, Nemser B, Ozcan A, Garner O, Di Carlo D, Ballard Z, Joung HA, Garcia-Romeu A, Griffiths RR, Baumgarth N, Fallon BA. 2021.

Recent progress in Lyme disease and remaining challenges. Front Med (Lausanne) 8:666554. https://doi.org/10.3389/fmed.2021.666554.

50. Wormser GP, Nadelman RB, Schwartz I. 2012. The amber theory of Lyme arthritis: initial description and clinical implications. Clin Rheumatol 31:989–994. https://doi.org/10.1007/s10067-012-1964-x.

51. Wei T, Simko V, Levy M, Xie Y, Jin Y, Zemla J. 2017. Package 'corrplot'. Statistician 56:e24.

52. Berman HM, Westbrook J, Feng Z, Gilliland G, Bhat TN, Weissig H, Shindyalov IN, Bourne PE. 2000. The Protein Data Bank. Nucleic Acids Res 28:235–242. https://doi.org/10.1093/nar/28.1.235.